COMPUTATION OF ATMOSPHERIC ENTRY FLOW ABOUT A LEONID METEOROID

IAIN D. BOYD
Department of Aerospace Engineering
University of Michigan, Ann Arbor, Michigan, USA
E-mail:iainboyd@engin.umich.edu

(Received 15 May 2000; Accepted 7 August 2000)

Abstract. The flow field is computed around a 1 cm diameter Leonid meteoroid as it enters the Earth's atmosphere at an altitude of 95 km and a velocity of 72 km/s. These conditions correspond to a Knudsen number of 4 and a Mach number of 270. To accurately compute the gas flow, these extreme nonequilibrium conditions require application of a kinetic approach and the present work employs the direct simulation Monte Carlo method. A meteoroid ablation model is included in the computations and is found to play a significant role. The computational results predict that a large region of the flow field is affected by meteoroid ablation that produces an extended wake at high temperature in a state of thermal equilibrium. These findings are in qualitative agreement with spectroscopic observations of the 1998 Leonid meteoroid shower. The computations indicate that the results are sensitive to the material properties assumed for the meteoroid.

Keywords: Ablation, atmospheric entry, meteoroid, rarefied gas dynamics

1. Introduction

Annual meteoroid showers such as the Leonids and the Perseids are of interest for a variety of reasons. It has been proposed that comets and meteoroids entering the Earth's atmosphere carried with them extraterrestrial chemical elements that were required to develop life on Earth. In addition, the passage of high velocity meteoroids through the atmosphere is believed to affect the overall aerothermochemistry. Also, there has been concern over the possible interference of Earth orbiting satellites by the increased rate of meteoroid impacts on the spacecraft that occurs during the showers. It is estimated that the Leonid showers of 1998 and 1999 were at the peak of the 33 year cycle, and no adverse effects have been reported for any spacecraft. However, the showers have raised the general issue of the need to understand this type of potential hazard.

As part of the international scientific study of the Leonids, NASA and the United States Air Force, in a collaborative effort, undertook two airborne flight experiments (one each in 1998 and 1999) called the Leonid Multi-Instrument Aircraft Campaigns (Leonid MAC). Details of these experiments are summarized by Jenniskens and Butow (1999).

Earth, Moon and Planets **82–83**: 93–108, 2000.

One of the instruments in the 1998 study was a high resolution slitless CCD spectrograph. The data from this instrument were surprising. The spectra were characterized by relatively high temperatures (about 4,300 K) based on both atomic lines and rotational band structure of molecules (Jenniskens *et al.*, 2000). It was surprising under the nonequilibrium conditions associated with entry of a Leonid meteoroid that the flow should be characterized by an elevated temperature in a state of thermal equilibrium.

In an attempt to help to understand these spectral observations, it is the primary goal of this study to compute the two dimensional flow field about a typical Leonid meteoroid entering the Earth's atmosphere. It will be found that the flow conditions provide very rarefied, hypersonic flow, and so the numerical method employed is the direct simulation Monte Carlo (DSMC) technique (Bird, 1994). This is believed to be the first attempt to apply the DSMC technique to a computation of this type. In the paper, the flow conditions and the properties of the meteoroid are first described. Then a brief description of the DSMC method and code employed are provided. Results of three different computations are presented and discussed. Areas where further work is needed are also considered.

2. Model of A Leonid Meteoroid

The physical properties of meteoroids in the Leonid shower are not well known. Here, we consider a representative case of a spherical meteoroid of diameter 1 cm, entering the Earth's atmosphere at an altitude of 95 km at a speed of 72 km/s. The standard atmospheric conditions at this altitude are as follows: number density of $N_2 = 2.8\times10^{19}$ m^{-3}, number density of $O_2 = 7.0\times10^{18}$ m^{-3}, number density of O $= 4.9\times10^{17}$ m^{-3}, temperature = 176 K. These conditions give a free stream Knudsen number (the ratio of mean free path to body diameter) of about 4, and a Mach number (the ratio of meteoroid velocity to the speed of sound) of 270. The high Knudsen number indicates that the gas flow around the meteoroid is almost collisionless. The high Mach number (this is ten times higher than that of the Space Shuttle as it enters the atmosphere) indicates that any collisions (either gas-gas or gas-surface) are extremely energetic. This clearly represents a very strong nonequilibrium flow condition. It is to be emphasized that this set of parameters is taken to be representative. In the showers, there are variations in meteoroid size, altitude, and velocity. The present investigation represents an initial attempt to see if a computational analysis of the flow field can provide any useful information.

Table I

Meteoroid Type	M_{meteor} (kg/kg-mol)	Q (kJ/g)
H-Chondrite	23.6	6.3
Comet (Halley)	8.26	3.8

It will be found in the computations that including ablation of the meteoroid due to interaction with the atmosphere is significant. This process can be modeled in a simple way following the approach described by Bronhsten (1983). In this model, the number of surface material atoms evaporated due to impact by an air molecule is given by:

$$N_{meteor} = \frac{M_{air} V_{air}^2}{2 M_{meteor} Q} \tag{1}$$

where M_{air} and V_{air} are the mass and velocity of the impacting air molecule, respectively, M_{meteor} is the mass of the meteoroid particle evaporated, and Q is the heat of vaporization. The parameters M_{meteor} and Q depend on the meteoroid material. There is uncertainty concerning the material of Leonid meteoroids. In this study, two different types of meteoroid are considered: (1) an H-chondrite meteoroid; and (2) a comet-like meteoroid (data from comet Halley are employed here). Leonids are generally assumed to consist of comet-like material. However, small Leonids may be depleted of volatiles due to solar irradiation, and in this case their composition may be closer to the chondritic one. These two meteoroid materials differ in their chemical composition giving rise to differences in average particle mass and heat of vaporization. The values used in this study are obtained from Jaroscewich (1990) and Jessberger, *et al.* (1988), and are listed in Table I.

In the flow field computation (described in detail below), each time a particle of any species impacts on the surface of the meteoroid, a number of vaporized particles given by Eq. 1 is introduced into the flow field from the meteoroid surface. The meteoroid vapor is assumed to be a single species with the average mass of the material (as listed in Table I). The heats of vaporization given in Table I correspond to a material temperature of 2,500 K and this is used as the surface temperature of the meteoroid.

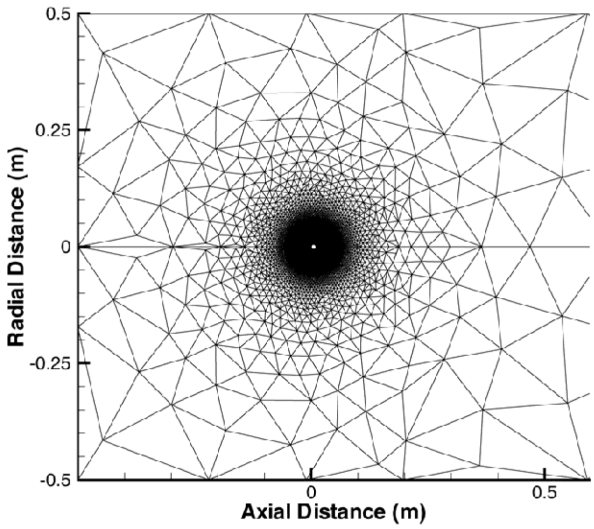

Figure 1. Close up view of the computational grid in the vicinity of the meteoroid.

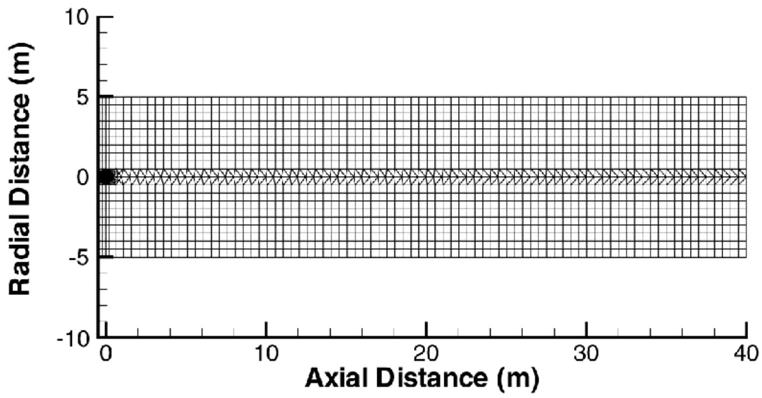

Figure 2. Computational grid for the complete flow field.

3. Model of the Flow Field

The highly rarefied nature of the flow under consideration suggests application of a kinetic based computational approach. In the present work, the direct simulation Monte Carlo method (DSMC) (Bird, 1994) is employed. This technique has been developed and applied to a variety of rarefied flows for many years. Some of its greatest successes have been in application to high altitude, hypersonic flows of spacecraft and missiles (Rault, 1994; Boyd, Phillips, and Levin, 1998). However, the meteoroid entry Mach number of 270 is at an unprecedentedly high level in comparison to these prior studies.

The DSMC technique uses model particles to emulate the motions and collisions of real molecules. Each particle represents a much larger number of actual atoms or molecules. The particles move through physical space over a time step that is smaller than the mean time between collisions. The particles are collected into computational cells that have dimensions of the order of the local mean free path. With such small cells, the assumption is made that the exact location of particles within the cell is negligible in deciding which particles in the cell may collide with one another. Therefore, pairs of particles are formed at random, and a probability of collision for each pair is computed based on the relative velocity of the pair, and the physical properties of the particles. Macroscopic properties are obtained from the microscopic particle properties by time averaging. A thorough description of the method and its application can be found in Bird (1994).

In the present work, a general DSMC code called MONACO (Dietrich and Boyd, 1996) is employed. MONACO offers great flexibility in terms of the computational grid through the use of unstructured, triangular cells. This is an important requirement for the computation of the flow fields around meteoroids due to the large dynamic range of density (and therefore mean free path, and therefore cell size) encountered in these flows. A close up view of the computational grid in the region close to the meteoroid is shown in Figure 1. The meteoroid is represented by the small circle near the middle of the image. The cells are tightly clustered around the meteoroid due to the fact that the total flow field density is found to increase significantly in this region. This is discussed further in the next section. The complete computational domain is shown in Figure 2. This grid was finalized after several low resolution computations.

The physical modeling for this initial study of meteoroid flows is kept to a relatively simple level. Air is represented by three chemical species (N_2, O_2, and O). The vapor ablated from the meteoroid surface is assumed to be a single chemical species with mass given by the values listed in Table I. Thermal relaxation is allowed between the translational, rotational, and vibrational energy modes. The Variable Hard Sphere (VHS) collision model is employed (Bird,1994) in which the collision cross section is given by:

$$\sigma = \sigma_{ref} \left(\frac{g}{g_{ref}} \right)^{1-2\omega} \tag{2}$$

where g is the relative velocity, a value of $\omega = 0.7$ is used for air, and σ_{ref} and g_{ref} are reference values. The reference collision diameter for these studies is 4 $\mathring{A}$. No chemical reactions are considered. All species

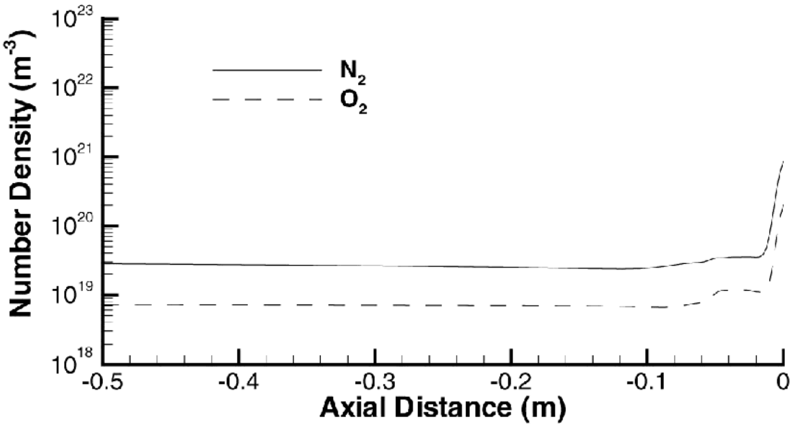

Figure 3. Profiles of number density along the stagnation streamline: no ablation.

are assumed to be in their ground electronic states. In reality, as will be seen, there are highly energetic collisions that occur immediately in front of the meteoroid that would lead to chemical reactions (in particular, molecular dissociation), electronic excitation, and ionization of the air species. Inclusion of these more detailed phenomena are left to future studies. It is expected that inclusion of chemical reactions will increase the number density of air species in the wake by close to a factor of two, assuming that all molecules are dissociated into atoms. The model for meteoroid ablation is described above. The properties of both the impacted particles after reflection and any ablated vapor particles are determined assuming diffuse reflection at the meteoroid surface temperature of 2,500 K.

4. Results and Discussion

Three different sets of computational results are presented. The first involves flow without any meteoroid ablation; and the second and third consider ablation of the two different types of meteoroid material listed in Table I. In all three cases the computational grid shown in Figure 2 is employed. The computations employ 2 million particles and are performed on four processors of an SGI Origin parallel computer in the Keck Computational Fluid Dynamics Laboratory at the University of Michigan. For the cases that include ablation, 30,000 iterations are required to reach steady state. The macroscopic results presented here are then obtained by sampling over a further 50,000 iterations. The total computation time for each case is about 18 hours.

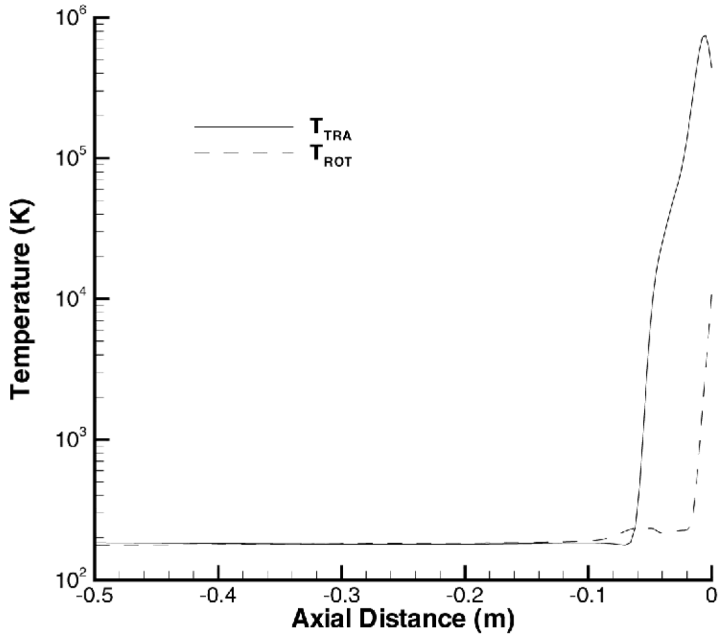

Figure 4. Profiles of temperature along the stagnation streamline: no ablation.

4.1. (1) Non-Ablating Meteoroid

In Figure 3, the number density profiles of molecular nitrogen and oxygen along the symmetry line in the region in front of the meteoroid (i.e. along the stagnation streamline) are shown. There is a significant rise in the densities of the air species immediately next to the body. This increase is due primarily to the fact that the body surface temperature is significantly smaller than the adiabatic stagnation temperature of this high speed flow. The profiles of translational and rotational temperature along this same line are shown in Figure 4. The translational temperature reaches a value of almost 1,000,000 K close to the surface. Note that the adiabatic stagnation temperature under these conditions is about 2,500,000 K. There are two important points to be made about this high temperature. The first is that under these strongly nonequilibrium conditions, the velocity distribution function will not have its equilibrium Maxwellian form. Therefore, the definition of temperature is unclear. In the DSMC method, the temperature computed represents a measure of the width of the overall velocity distribution function. Along the stagnation streamline, the velocity distribution function contains two distinct populations. One originates in the free stream, and is characterized by a low temperature (176 K) with a large off-set from zero (72 km/s). The second population consists of molecules

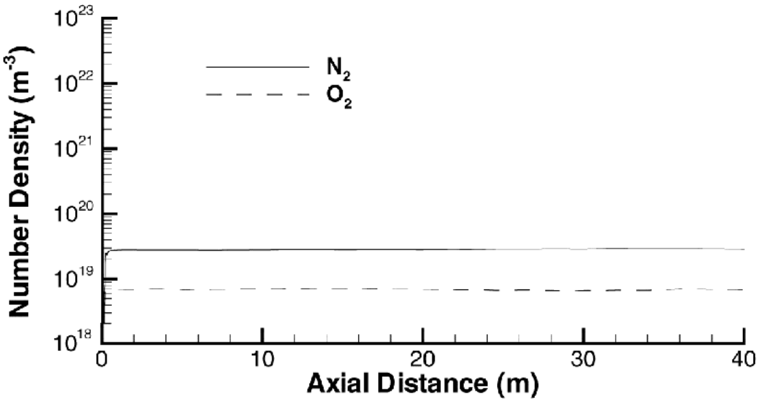

Figure 5. Profiles of number density along the wake centerline: no ablation.

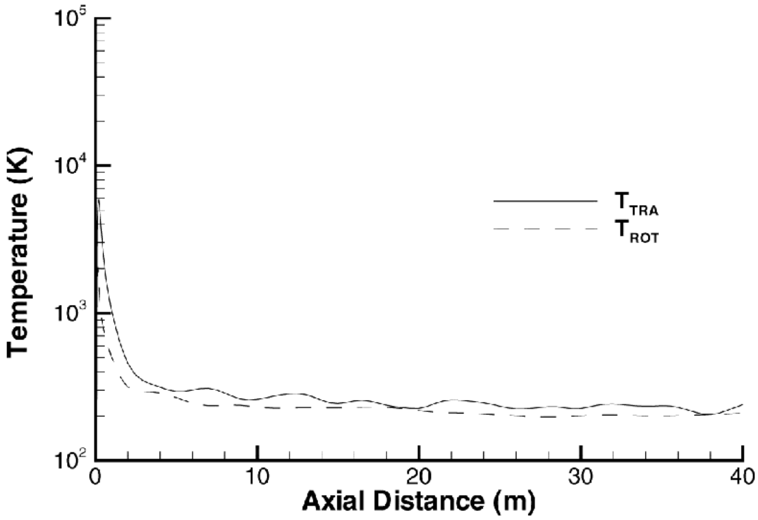

Figure 6. Profiles of temperature along the wake centerline: no ablation.

reflected from the meteoroid surface that are characterized by a higher temperature (2,500 K) and a lower, negative velocity (-1 km/s). The width of the overall distribution may be large, but almost no molecules are characterized by this temperature in the thermal sense. The second point is that these large temperatures may be somewhat reduced in the real flow through inelastic collision events such as dissociation, ionization, and electronic excitation.

In Figures 5 and 6 the species number densities and temperatures along the symmetry line behind the meteoroid (i.e. in the wake) are shown. The number densities are constant at their free stream values. The temperatures rapidly decrease to their free stream values from the

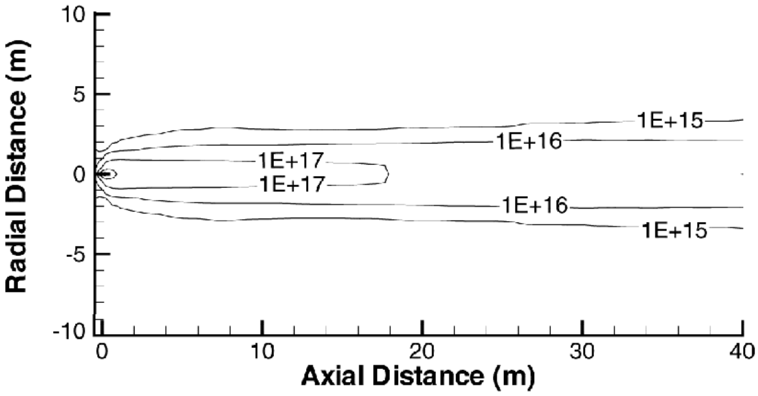

Figure 7. Contours of the number density of ablated vapor: H-chondrite meteoroid.

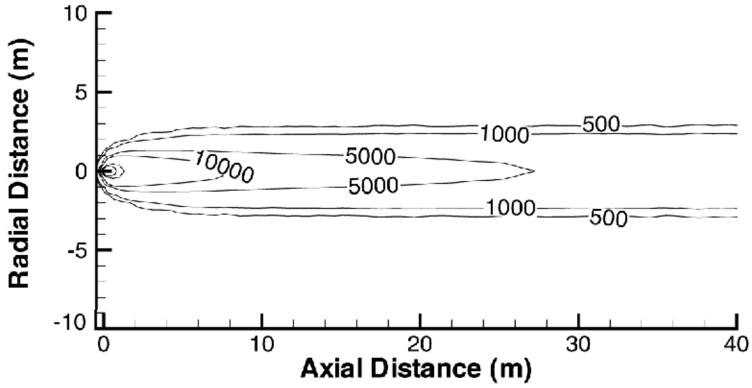

Figure 8. Contours of translational temperature: H-chondrite meteoroid.

elevated levels generated in front of the meteoroid. The translational and rotational modes are close to being in thermal equilibrium.

These results do not show the behavior found in the MAC spectroscopic investigations of the 1998 Leonid shower. This suggests that meteoroid ablation may provide an important mechanism in generating the high temperature, thermal equilibrium region that was observed.

4.2. (2) H-Chondrite Meteoroid

Before performing the computations, it is clear that a significant amount of ablation should occur in these flows using the simple evaporation model, Eq. 1. Each air molecule impacting at the free stream velocity on the H-chondrite meteoroid is predicted to ablate about 500 meteoroid particles. Of course, as ablation proceeds, a cloud of ablated vapor surrounds the meteoroid, and it becomes less likely for air molecules to strike the meteoroid directly. Therefore, a steady state is eventually

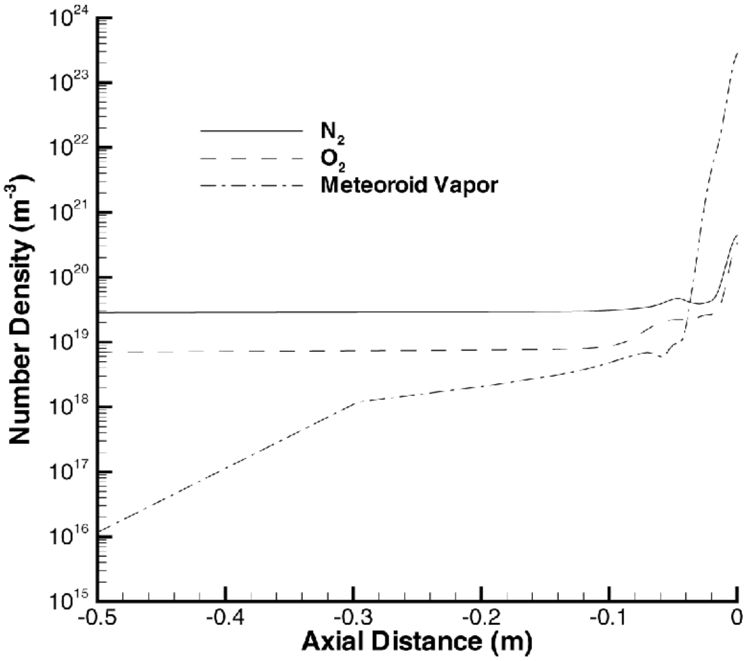

Figure 9. Profiles of number density along the stagnation streamline: H-chondrite meteoroid.

reached which forms a stable vapor cloud that expands rapidly away from the meteoroid. In Figure 7, contours of the number density (in m^{-3}) of meteoroid vapor are shown for the entire computational domain. A cylindrical wake with a waist diameter of about 6 m extends far behind the meteoroid. The corresponding translational temperature contours (in K) are shown in Figure 8. Due to the significantly higher densities of the air species within most of the meteoroid trail, these translational temperatures represent those of the air species. The meteoroid ablation leads to a large region of high temperature air in the wake of the meteoroid with values of several thousand degrees.

The species number densities and temperatures along the stagnation streamline are shown in Figures 9 and 10, respectively. The very high density cloud of meteoroid vapor in front of the body is clearly shown in Figure 9. The peak density of the vapor is more than two orders of magnitude higher than the peak density of the air species. The mean free path of the flow immediately adjacent to the meteoroid is about 10^{-5} m giving a local Knudsen number based on the meteoroid diameter of 0.001 which is in the near-continuum regime. The large range of Knudsen number encountered in the flow field requires use of sub-cells in the DSMC computation to adequately resolve the collisional behavior

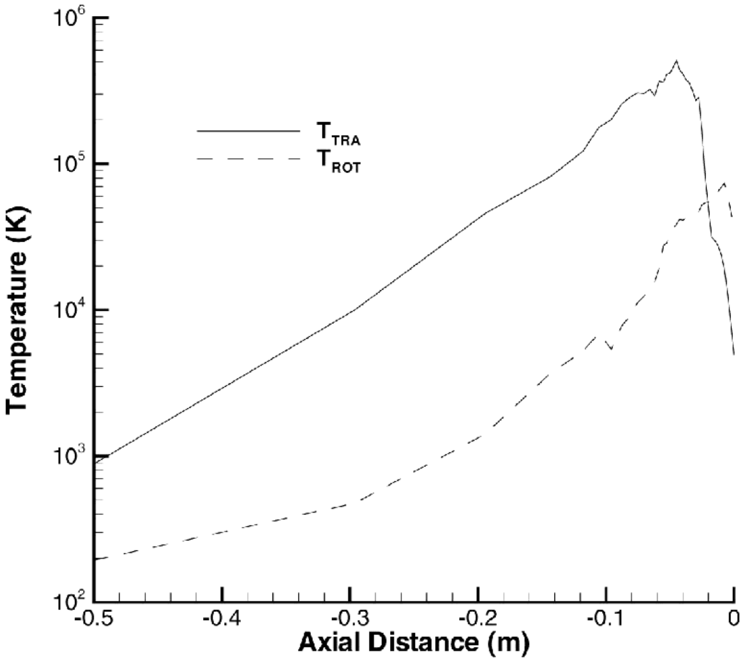

Figure 10. Profiles of temperature along the stagnation streamline: H-chondrite meteoroid.

close to the body. Far away from the meteoroid, the density of the ablated vapor decays rapidly. In comparison with the temperature profiles shown in Figure 4 for the case without ablation, the results provided in Figure 10 indicate that the rise in temperature occurs over a much larger spatial region. Again, caution is needed in the interpretation of translational temperature. The results in Figure 10 are an indication of the width of the velocity distribution function in a multi-species, strongly nonequilibrium environment.

The structure of the flow field behind the meteoroid is considered in Figsures 11 and 12 which show the number density and temperature profiles along the centerline in the wake flow downstream of the meteoroid. Here it is found that the air species densities are almost identical to the case without ablation, and the density of the ablated material slowly decays. The temperatures rapidly decay immediately behind the meteoroid and then slowly decrease with distance. The temperatures far behind the meteoroid are significantly higher than those computed for the no ablation case. It is significant to note that the computations including meteoroid ablation predict temperatures of several thousand degrees with the translational and rotational modes in thermal equilib-

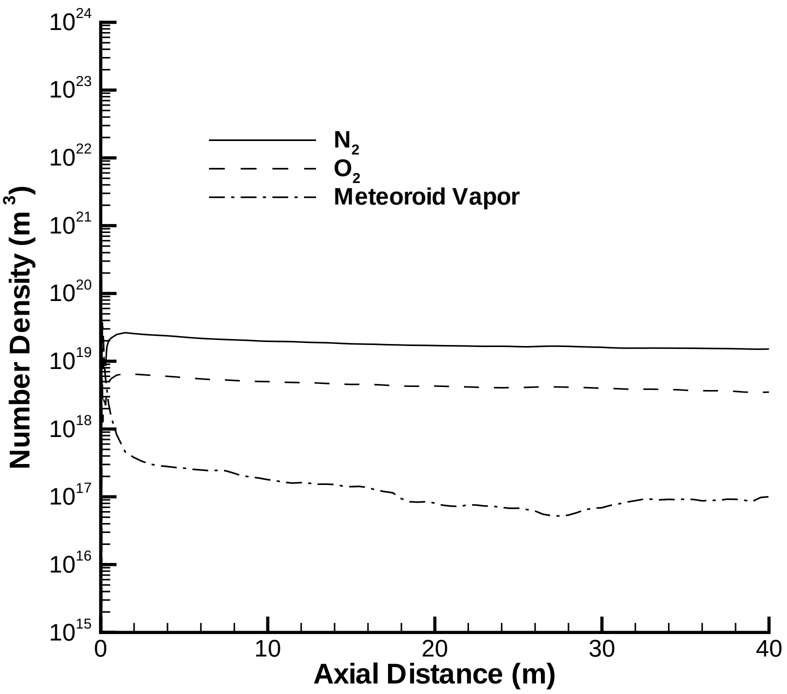

Figure 11. Profiles of number density along the wake centerline: H-chondrite meteoroid.

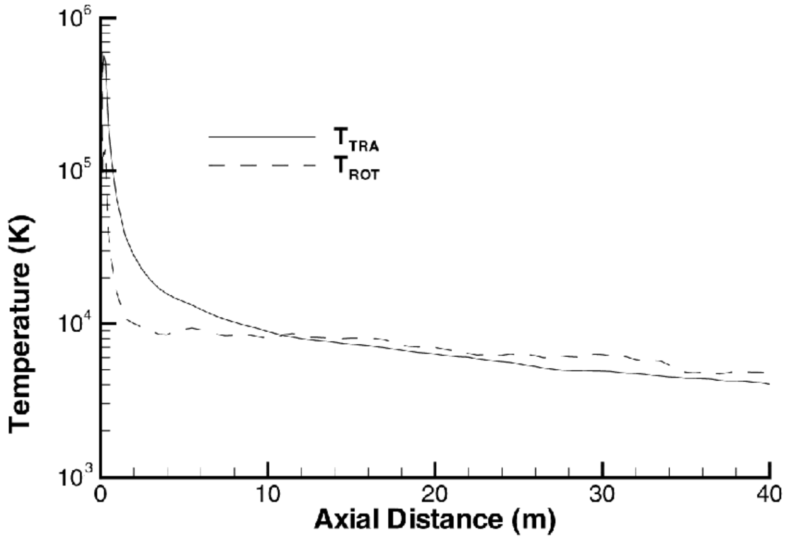

Figure 12. Profiles of temperature along the wake centerline: H-chondrite meteoroid.

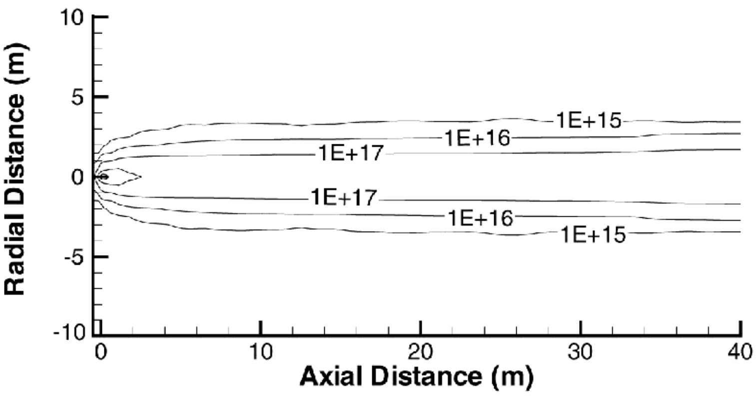

Figure 13. Contours of the number density of ablated vapor: comet-like meteoroid.

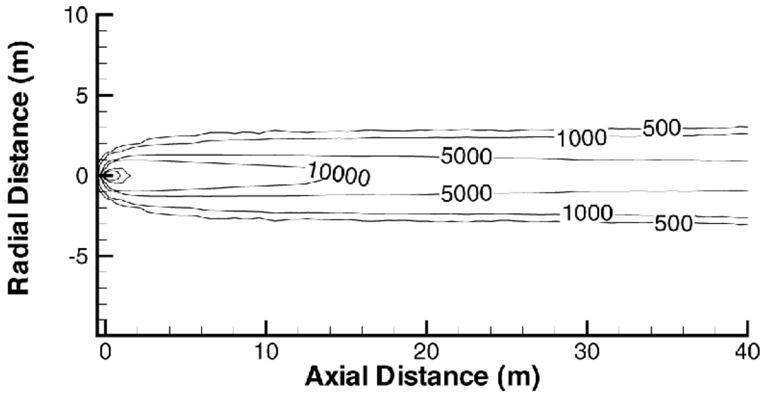

Figure 14. Contours of translational temperature: comet-like meteoroid.

rium. These characteristics of the results are in qualitative agreement with the airborne spectral measurements.

4.3. (3) Comet-like Meteoroid

To investigate the sensitivity of the results shown in Figures 7–12, the meteoroid material is changed to the comet-like substance with properties as listed in Table I. Flow field contours of the number density of the ablated meteoroid vapor and of translational temperature are shown in Figures 13 and 14, respectively. As might be expected, there are some changes to the wake structure. The properties of the comet-like material result in the ablation of about 2,350 meteoroid particles for each impact of a free stream air molecule on the surface. This increase in the number of ablated particles is in part due to the lighter mass of the comet-like material and this will also lead to a greater degree

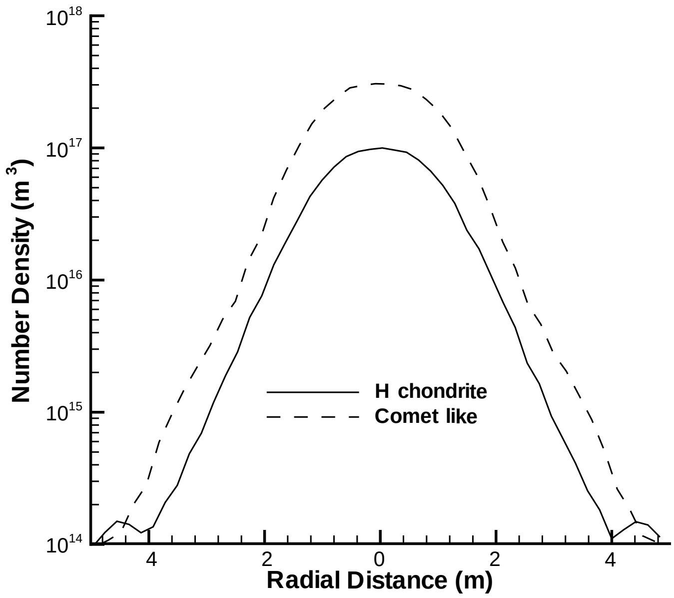

Figure 15. Radial profiles of ablated vapor number density at 20 m behind the me teoroid.

of diffusion of the meteoroid vapor through the surrounding air. These characteristics are seen in the flow field contours. The number density of ablated vapor in the wake is higher for the ablation of comet-like material and the translational temperature is also higher.

It is found that the profiles of the species densities and the temperatures of the different energy modes along the stagnation streamline and the wake streamline are similar for this case to those shown in Figures 9 through 12. Comparisons of the results for the two different meteoroid materials are compared in Figures 15 and 16, where radial profiles at a distance of 20 m behind the body are shown for ablated vapor number density and translational temperature. The density of ablated material is at least a factor of three higher than for the H-chondrite meteoroid for most of the profile. The translational temperature for the comet-like case is about 2,000 K higher on the centerline.

5. Conclusions

The direct simulation Monte Carlo method was employed to compute the two-dimensional flow field around an ablating meteoroid. The properties of the body were representative of a Leonid meteoroid. It was found that a simple ablation model led to the formation of an exten-

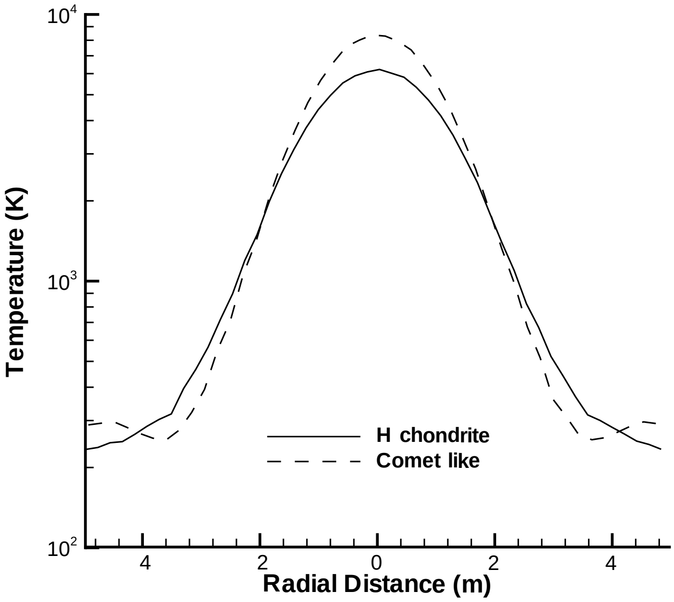

Figure 16. Radial profiles of translational temperature at 20 m behind the meteo roid.

ded, high temperature wake of several thousand degrees behind the meteoroid. Due to the build up of ablated vapor around the meteoroid, there was a sufficient number of intermolecular collisions to maintain the gas in the wake in a state of thermal equilibrium. These findings of the computational study were in qualitative agreement with air-borne spectrographic measurements. It is therefore concluded that this type of computational analysis can aid greatly in the understanding of meteoroid ablation phenomena.

One of the most important predictions from the computations is the physical size of the meteoroid trail. In the present study, a waist diameter of 6 m is predicted. Observations of different meteoroids give a wide range of sizes. For example, radiometeor data indicate initial radii of meteor trains in the range of 2 to 7 m (Ceplecha, *et al.*, 1998). Photographs of fast meteors show trail lengths of 50 to to 150 m (Babadzhanov and Kramer, 1968). Of course, the trail size will vary with meteoroid altitude, velocity, size, and composition. Assessment of the present computer predictions requires further experimental study to carefully characterize the luminous volume of meteoroid trails for which spectra are measured.

As stated at the beginning, this study is preliminary in nature. While the main goals of the investigation were achieved, it is clear that much work is required to improve the physical modeling included in the computations. For example, there is the need to include dissociation and ionization reactions of the air species colliding at very high energy with ablated meteoroid vapor. In addition, there is the need to improve the meteoroid ablation model to include more microscopic phenomena.

In addition to improving the physical modeling, there is a need to understand the sensitivity of the computational results to the flow conditions considered. In particular, computations should be performed for variations in the meteoroid size, altitude, and velocity. Attempts should be made to use the flow field results to compute synthetic spectra for direct comparison with the airborne data measured during the Leonid MAC.

Acknowledgements

The author expresses his gratitude to Peter Jenniskens, Olga Popova, and Christophe Laux for extremely helpful discussions during this study. Funding was provided in part by the NASA Exobiology program through a grant with the SETI Institute. The computations were performed on an SGI Origin 2000 funded by AFOSR grant F49620-99-1-0164 with Dr. Marc Jacobs as monitor. *Editorial handling:* Noah Brosch.

References

Babadžanov, P. B. and Kramer, E. N.: 1968, in L. Kresak and P.M. Millman (eds.), *Physics and Dynamics of Meteors*, p. 128–142.

Bird, G. A.: 1994, *Molecular Gas Dynamics and the Direct Simulation of Gas Flows*, Oxford University Press, 458 pp.

Boyd, I. D., Phillips, W.D., and Levin D.A.: 1998, *Journal of Thermophysics and Heat Transfer* **12**, 38–44.

Bronshten, V. A.: 1983, *Physics of Meteoric Phenomena*, D. Reidel Publ. Co., Dordrecht, 356 pp..

Ceplecha, Z., Borovička, J., Elford, W.G., ReVelle, D.O., Hawkes, R.L., Porubcan, V., and Simek, M.: 1998, *Space Science Reviews* **84**, 327-471.

Dietrich, S. and Boyd, I.D.: 1996, *Journal of Computational Physics* **126**, 328–342.

Jaroscewich, E.: 1990, *Meteoritics* **25**, 323–337.

Jenniskens, P. and Butow, S.J.: 1999, *Meteoritics Planet. Sci.* **34**, 933–943.

Jenniskens, P., Packan, D., Laux, C., Wilson, M., Boyd, I.D., Popova, O., Krueger, C.H., and Fonda, M.: 2000, *Earth, Moon and Planets* **82–83**, 57–70.

Jessberger, E. K., Christoforidis, A., and Kissel, J.: 1988, *Nature* **332**, 691–695.

Rault, D.F.G.: 1994, *Journal of Spacecraft and Rockets* **31**, 944–952.